

Discrete Latent Graph Generative Modeling with Diffusion Bridges

Van Khoa Nguyen^{1,2} Yoann Boget^{1,2} Frantzeska Lavda^{1,2} Alexandros Kalousis^{1,2}

Abstract

Learning graph generative models over latent spaces has received less attention compared to models that operate on the original data space and has so far demonstrated lacklustre performance. We present GLAD a latent space graph generative model. Unlike most previous latent space graph generative models, GLAD operates on a discrete latent space that preserves to a significant extent the discrete nature of the graph structures making no unnatural assumptions such as latent space continuity. We learn the prior of our discrete latent space by adapting diffusion bridges to its structure. By operating over an appropriately constructed latent space we avoid relying on decompositions that are often used in models that operate in the original data space. We present experiments on a series of graph benchmark datasets which clearly show the superiority of the discrete latent space and obtain state of the art graph generative performance, making GLAD the first latent space graph generative model with competitive performance. Our source code is published at: <https://github.com/v18nguye/GLAD>

1. Introduction

Graph generation has posed a longstanding challenge. A versatile range of solutions have been proposed over time, from simple models (Erdős et al., 1960; Albert & Barabási, 2002) to more recent deep generative models (Jo et al., 2022; Vignac et al., 2023; Kong et al., 2023). Within that latter approach the landscape of existing methods is rich and complex. To navigate this landscape we will start by a characterisation of the existing methods along two dimensions: the representation space over which the generative models are learnt, latent versus observed, and how the graph generation is done, autoregressively versus one-shot.

¹Geneva School for Business Administration (HES-SO)
²Department of Computer Science, University of Geneva, 1214 Geneva, Switzerland. Correspondence to: Van Khoa Nguyen <van-khoa.nguyen@etu.unige.ch>.

Preprint. Under review.

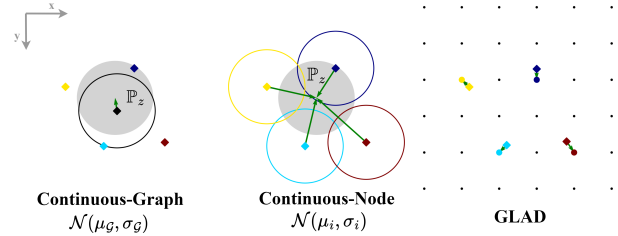


Figure 1. Latent spaces for graphs: (Left) *Continuous-graph latent space*: We encode a graph as a distribution (black circle) defined over the pooled representation (black diamond) of its node embeddings (colored diamonds), and regularised towards the normal prior \mathbb{P}_z (grey disk). (Middle) *Continuous-node latent space*: We encode a graph as a product of latent node distributions (colored circles), each regularized towards the normal prior \mathbb{P}_z . (Right) *Quantised discrete-node latent space*: GLAD encodes a graph as a set of node embeddings (colored dots) allowed to take values only over uniformly quantised latent space (black dots). Unlike the two continuous latent spaces this one preserves the discrete nature of the embedded objects.

When it comes to the graph representation space most state-of-the-art methods operate over the original data space and learn generative models over node and edge features (Shi et al., 2020; Luo et al., 2021; Jo et al., 2022; Kong et al., 2023; Vignac et al., 2023), showcasing a flexible adaptation to learning over discrete representations. Less attention has been given to methods that operate over graph latent spaces and the appropriate definition and design of such latent spaces. Some initial efforts (Simonovsky & Komodakis, 2018; Jin et al., 2018; Liu et al., 2018; Samanta et al., 2020) propose learning the graph distribution over the latent space of variational autoencoders (VAEs) (Kingma & Welling, 2013). Yet, such approaches often suffer from high reconstruction errors, have to solve challenging graph-matching problems, and/or rely on heuristic corrections for the generated graphs.

Graph generation can be either auto-regressive or one-shot. Auto-regressive models generate samples one graph element at the time operating over basic structural components of the graphs, e.g. nodes, edges or substructures, (You et al., 2018a; Shi et al., 2020; Luo et al., 2021), and rely on the availability of an ordering of the graph elements. While these models have demonstrated promising results and over-

come the likelihood intractability, by the very fact that they require an order they do not provide a principled way to learn graph distributions in a permutation-invariant manner. Consequently, they make away with the permutation invariance by resorting to heuristic orderings (You et al., 2018a; Shi et al., 2020; Luo et al., 2021) or employ learning approaches to partially address the limitation (Chen et al., 2021).

One-shot graph generative models and in particular diffusion-based models, have recently emerged as a very compelling approach for modeling graph distributions (Niu et al., 2020; Jo et al., 2022; Vignac et al., 2023). They allow for the natural incorporation of the permutation-equivariance property as an inductive bias within their denoising component. Obviously they are not without limitations. The initial graph diffusion methods rely on continuous score functions to model the graph distributions. They learn these score functions by denoising graph structures that have been noised with real-valued noise (Niu et al., 2020; Jo et al., 2022). Continuous score functions are a poor match for structures that are inherently discrete. Note that similar caveats also appear in VAE-based approaches where the graph latent representations are constrained to follow the standard normal distribution (more on that on Section 2.1) There are some diffusion-based works that treat graphs heads-on as discrete objects (Vignac et al., 2023). In addition, constructing appropriate score functions over the original graph representation is challenging. Common approaches factorise these score functions to node- and adjacency-matrix-specific components which require their own distinct denoising networks. These partial score functions provide a fragmented view of the graph and do not reflect well the true score function making them a poor choice to model graph distributions. Note that such decompositions are used both in the continuous diffusion-based approaches for graphs as well as in the discrete ones. Diffusion-based models typically have a denoising component which operates over the edges. The denoising process takes place over densely(fully)-connected graphs (Niu et al., 2020; Jo et al., 2022; Vignac et al., 2023); this poses significant scalability challenges for larger graphs such as social networks (Wang et al., 2018).

In this work we start from certain desiderata that a graph generative model should satisfy, which will guide the design of our model. Graph generative models should learn graph distributions that are node permutation invariant. Graphs should be treated in a holistic manner without relying on artificial decompositions to their components. Finally graphs should be treated as discrete objects, as they are. To address these desiderata we propose **Graph Discrete Latent Diffusion (GLAD)** a generative model that operates on a carefully designed permutation-equivariant discrete latent space that models graphs in an holistic manner, while

explicitly accounting for their discrete nature. We will do generation using a one-shot approach, relying on Graph Neural Network for encoding and decoding, from and to the latent space, satisfying also the permutation equivariance desiderata. Our latent space ensures efficient graph encoding and supports highly accurate reconstructions. GLAD extends diffusion bridges (Heng et al., 2021; Peluchetti, 2022), and in particular (Liu et al., 2023) proposed for constrained data domains, to the domain of graphs by operating over our graph latent space. We carefully evaluate our method on a set of graph benchmarks and compare its performance against that of state-of-the-art generative methods for graphs. GLAD consistently outperforms the baselines validating the merits of our discrete latent diffusion bridge and its capacity to model complex dependencies in graph structures. We summarise our key contributions as follows:

- We present a simple, yet powerful, quantised discrete latent space for graphs building on finite element quantisation (Mentzer et al., 2023) which delivers significantly better reconstruction compared to previous methods that operate on continuous latent spaces.
- We introduce a new generative model for graphs that tailors diffusion bridges to our discrete latent space; our model does not resort to component specific decompositions and is permutation-invariant.
- GLAD is the first approach for one-shot diffusion-based graph generative modelling over a discrete latent space. We demonstrate a robust and consistently better generative performance against state-of-the-art methods across a number of graph generation benchmarks.

2. Background

We use a tuple $\mathcal{G} = (X, E)$ to denote the spatial structure of a graph, where X and E are node, edge (adjacency) matrices, respectively. When it comes to representing graphs for generative modelling there are two main approaches. In the first, we directly operate in the original graph representation as it is given by the \mathcal{G} tuple, i.e. over the original nodes and edges representations and features, and learn the generative model over it.

Alternatively we can define appropriate latent spaces for graphs and learn the generative models over them. Concretely, under the latent-space approach graphs are first encoded by an encoder, ϕ , to some latent space which is governed by a distribution q_ϕ . Subsequently a decoder, θ , maps the latent space encodings back to the original space governed by the generative distribution p_θ . The very nature of graphs makes it that there are different ways of encoding them to a latent space. A popular choice is to model a graph as the set of its node embeddings to some latent

space. We will denote that set as $Z = \{z_1, \dots, z_n\}$, where n is the total number of nodes and $z_i \in \mathbb{R}^{d_z}$ is the latent embedding of the i node. These embeddings are usually produced by graph neural networks and encode information not only about the node itself but also about its local neighborhood, essentially providing a description of a subgraph that is centered at the node i . Representing a graph as a set of node embeddings will be also our starting point towards the design of a latent space that satisfies the desiderata that we discussed in the introductory section.

2.1. Latent Graph Representation

When learning functions over graphs we need to consider whether these need to be node permutation invariant or equivariant. Informally, a graph function is permutation invariant if any permutation of its input leaves the output unchanged and equivariant when for any given permutation of the input the output is permuted in the same manner. We want to learn graph distributions in a manner that is node permutation invariant, in the sense that random node permutations of the training set graphs leave the learnt distribution unaffected. To that end the components of our model will have to be node permutation equivariant.

Handling graph invariances when learning latent graph representations for generative modeling is challenging. [Simonovsky & Komodakis \(2018\)](#) used Variational Autoencoders (VAEs) to model graph distributions. They establish the latent space using GNNS to learn the set of node embeddings Z , whose elements they then pool to obtain a global latent graph representation $z_{\mathcal{G}} = \oplus(Z)$, \oplus denotes the pooling operation. They constrain the graph latent distribution $q_{\phi}(z_{\mathcal{G}}|\mathcal{G})$, to follow a standard normal distribution. We will call such a latent space a continuous-graph latent space. Pooling operations are not permutation equivariant and one needs to solve a graph-matching problem on the decoding side to establish the reconstruction loss, which is computationally expensive and inaccurate. One way to avoid the need for solving a graph-matching problem is by resorting to the use of a canonical ordered graph representation such as a sequence- or a tree-based representation ([Jin et al., 2018](#)). Such approaches suffer from the fact that canonical representations are not unique for a given graph and as a result learning is not efficient. We summarise this discussion in the following observation.

Observation 2.1. *Global latent graph representations do not capture well the graph equivariance. The induced decoding distributions are not invariant to node permutations.*

Another way to alleviate the issues that are created by a global graph latent representation is simply to avoid pooling of the node embeddings altogether and operate over a latent representation that has a set structure. Such an approach is followed in different VAE-based methods, ([Liu et al., 2018](#);

[Samanta et al., 2020](#)). Since now the latent representation is the set of the node embeddings in the decoding step there is no ambiguity, we know the node correspondences, and thus no need to solve the graph matching problem. Unlike the case of canonical representations such an approach is by construction node permutation equivariant. These approaches will typically describe the latent space distribution using a decomposition over the latent node embeddings: $q_{\phi}(Z|\mathcal{G}) = \prod_i q_{\phi}(z_i|\mathcal{G})$ and regularise each of the latent node representations towards a standard normal distribution. We will call such a latent space a continuous-node latent space. Thus the latent representations of different nodes of a graph are assumed to have the same prior distribution. We illustrate a cartoon version of this assumption in the middle graph of [Figure 1](#). This simplistic assumption has a detrimental effect on accurate graph reconstruction as we will empirically demonstrate.

Observation 2.2. *Constraining the node latent representation to the same prior makes them less distinguishable from each other hindering the downstream decoding process.*

The above works model graph and node embeddings as normal distributions, making the assumption that the embedded structures lie in a continuous space with support everywhere; this is a simplistic assumption. A node encoding contains information about the node itself and the graph neighborhood (subgraph) within which the node lives. These are essentially discrete structures and while there are exponentially many different possibilities with the neighborhood size these are countable and inherently discrete. The appropriate way to model distributions over such objects is by treating the latent spaces as discrete and use discrete distributions. There is a rather limited number of works that treat the problem of graph latent generative modelling as a discrete problem and operate over discrete spaces and discrete distributions. Notable exceptions to that are: discrete flows for graphs (GraphDF) ([Luo et al., 2021](#)) and Vector-Quantised Graph Auto-Encoder (VQ-GAE) ([Boget et al., 2023](#)). GraphDF is an autoregressive flow-based model, it traverses the graph elements in breadth-first manner, and operates over discrete latent node and edge structures. VQ-GAE, similar to GLAD, uses a permutation-equivariant graph auto-encoder to represent graphs as sets of node embeddings to a discrete, quantized, space. However unlike GLAD, which models the latent space distribution in a permutation-invariant manner, VQ-GAE learns it auto-regressively, by establishing an ordering over the set of node embeddings.

Observation 2.3. *Graph latent spaces should be discrete and modelled using discrete distributions in order to faithfully represent the discrete nature of graphs.*

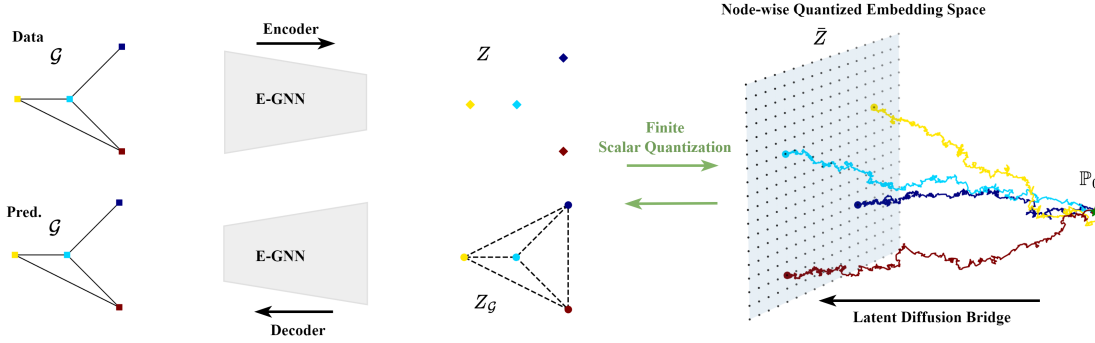


Figure 2. **Overview of GLAD** An equivariant GNN (E-GNN) encodes a graph as a set of continuous latent node embeddings, colored diamonds. The quantisation operator maps these embeddings to points on a uniform discrete grid, colored circles. An E-GNN decoder reconstructs the graph from the set of the discrete node embeddings. We use diffusion bridges to learn the prior over the discrete space by diffusing from a fixed point prior, green star, to the conditioned discrete latent graph structure.

2.2. Diffusion Bridges on Structured Domains

We briefly present diffusion bridges (Heng et al., 2021; Peluchetti, 2022; Liu et al., 2023), which apply to structured domains. A diffusion bridge is a conditional stochastic process that ensures that the diffusion process converges to a given conditioning sample at the terminal state. The reachability of the conditioning sample is guaranteed by the *Doob’s h transform* (Doob & Doob, 1984). Let $\mathbf{Z} = \{Z_t : t \in [0, T]\}$ be a non-conditional diffusion process where the dynamics of the state $Z_t \in \mathbb{R}^d$ are characterized by the stochastic differential equation:

$$\mathbb{Q} : dZ_t = \eta(Z_t, t)dt + \sigma(Z_t, t)dW_t \quad (1)$$

W_t is a Wiener process, $\sigma : [0, T] \times \mathbb{R}^d \mapsto \mathbb{R}$ is a diffusion coefficient, and $\eta : [0, T] \times \mathbb{R}^d \mapsto \mathbb{R}^d$ is a drift function. Following the development in (Liu et al., 2023) we start by introducing the x -bridge: $\mathbb{Q}^x(\cdot) := \mathbb{Q}(\cdot | Z_T = x)$, where the conditioning factor that should be reached at the terminal state Z_T is the x sample. The x -bridge dynamics are given by a stochastic differential equation that is derived from the *h-transform* (Oksendal, 2013):

$$\mathbb{Q}^x : dZ_t = \eta^x(Z_t, t)dt + \sigma(Z_t, t)dW_t \quad (2)$$

The x -bridge’s drift is defined as $\eta^x(Z_t, t) = \eta(Z_t, t) + \sigma^2(Z_t, t)\nabla_{Z_t} \log q_{T|t}(x|Z_t)$; $q_{T|t}(x|Z_t)$ is the probability density of obtaining x at time T when we have Z_t at time t and $\nabla_{Z_t} \log q_{T|t}(x|Z_t)$ acts as a steering force towards x ; The steering force is central to guiding Z_t towards the specified target $Z_T = x$.

Given the x -bridge definition we can now construct a bridge process on a data distribution Π that is constrained over a discrete domain Ω . We call this bridge process a Π -bridge and denote it by \mathbb{Q}^Π ; Π -bridges will allow us to model distributions over constrained domains. \mathbb{Q}^Π is given by a

mixture of x -bridges; their end-points are conditioned on data samples $\{x^{(i)}\}_1^N$ i.i.d drawn from the data distribution Π . The dynamics of the Π -bridge $\mathbb{Q}^\Pi(\cdot) := \mathbb{Q}(\cdot | Z_T \in \Omega)$ are governed by the following stochastic differential equation:

$$\mathbb{Q}^\Pi : dZ_t = \eta^\Pi(Z_t, t)dt + \sigma(Z_t, t)dW_t \quad (3)$$

The Π -bridge’s drift is $\eta^\Pi(Z_t, t) = \eta(Z_t, t) + \sigma^2(Z_t, t)\mathbb{E}_{x \sim q_{T|t, \Omega}}[\nabla_{Z_t} \log q_{T|t}(x|Z_t)]$, where x is sampled from a truncated transition probability density given by $q_{T|t, \Omega}(x|Z_t) := q(Z_T = x | Z_t, Z_T \in \Omega)$. As we can see, the structured domain Ω is taken into consideration in the expectation of the steering forces. The marginal distribution, \mathbb{Q}_T^Π , induced by the Π -bridge at $t = T$ will match the data distribution Π by construction, i.e. $\mathbb{Q}_T^\Pi = \Pi$.

We want to learn a bridge model, \mathbb{P}^ψ , of the \mathbb{Q}^Π bridge. The learned bridge will generalise from the \mathbb{Q}^Π bridge and allow us to generate new samples from the Π distribution. We construct \mathbb{P}^ψ by learning a parametric drift function with a neural network. The dynamics of \mathbb{P}^ψ are given by:

$$\mathbb{P}^\psi : dZ_t = \eta^\psi(Z_t, t)dt + \sigma(Z_t, t)dW_t, \quad Z_0 \sim \mathbb{P}_0 \quad (4)$$

where $\eta^\psi(Z_t, t) = \sigma(Z_t, t)f_\psi(Z_t, t) + \eta^\Pi(Z_t, t)$, f_ψ is a parametric neural network, and \mathbb{P}_0 is a bridge prior. The Π -bridge \mathbb{Q}^Π imputes noise to data samples at different time steps which we use to learn the model bridge \mathbb{P}^ψ . We train \mathbb{P}^ψ by minimizing the Kullback-Leibler divergence between the two probability path measures $\min_\psi \{\mathcal{L}(\psi) := \mathcal{KL}(\mathbb{Q}^\Pi || \mathbb{P}^\psi)\}$; the Girsanov theorem, (Lejay, 2018), allows us to compute the \mathcal{KL} divergence with the following closed form solution:

$$\mathcal{L}(\psi) = \mathbb{E}_{Z_0 \sim \mathbb{P}_0, x \sim \Pi, t \sim [0, T], Z_t \sim \mathbb{Q}^x} [\|f_\psi(Z_t, t) - \bar{\eta}(Z_t, t)\|^2] \quad (5)$$

with $\bar{\eta}(Z_t, t) = \sigma^{-1}(Z_t, t)(\eta^x(Z_t, t) - \eta^\Pi(Z_t, t))$, where η^x, η^Π are introduced in Equation 2 and Equation 3, respectively. Equation 5 will become our training objective. We will use diffusion-bridges to learn graph generative models over a discrete graph latent space.

3. GLAD: Graph Discrete Latent Diffusion Model

We will now present GLAD our discrete latent diffusion-bridge model for graphs. GLAD has two components. We first define a discrete latent space for graphs, Section 3.1, and then show how to learn a prior over this latent space using diffusion-bridges, Section 3.2, which will allow us to do generation. We provide a high level view of GLAD in Figure 2.

3.1. Graph Equivariant Discrete Latent Space

We drive the design of the latent space by: i) ensuring that we learn distributions that are invariant to permutations, ii) encoding nodes and their local structures by ensuring that structural differences are reflected in the encoding, and iii) preserving the discrete nature of the objects we encode, nodes and their neighborhoods, and that of the graph itself.

Our graph latent representation will be a set of discrete latent embeddings of its nodes; unlike VQ-GAE (Boget et al., 2023), which uses learned vector-quantized representations, we derive these discrete embeddings using finite scalar quantization, (Mentzer et al., 2023); this produces a high dimensional quantized latent space in which nodes are embedded. Since we will not constrain the latent space, other than the quantization operation, it preserves to a significant extent the structural differences of the nodes and their neighborhood and at the same time it can encode very diverse local structures. We empirically verify these statements by demonstrating robust reconstruction performance across various graph benchmark datasets.

Concretely, we use a GNN encoder, ϕ , to first map a graph to a set of continuous node embeddings $Z = \phi(\mathcal{G}) = \{z_1, \dots, z_n\}$. The GNN encoder essentially pushes in the node encoding information about itself and its local neighborhood. We subsequently apply a quantization operator, \mathcal{F} , on the continuous node embeddings and map them to fixed points within the same space. The quantization operates independently on each dimension of the latent space, and the quantization of the j^{th} dimension of z_i embedding is given by:

$$z_{ij}^q = \mathcal{F}(z_{ij}, L_j) = \mathcal{R}\left(\frac{L_j}{2} \tanh z_{ij}\right), 1 \leq j \leq d_Z \quad (6)$$

where \mathcal{R} is the rounding operator ¹ and L_j is the number of

¹To ensure end to end differentiability we implement \mathcal{R} with

quantization levels used for the j^{th} dimension of the node embeddings. The quantisation operator maps any point in the original continuous latent space to a point from the set $\bar{Z} = \{\bar{z}_1, \dots, \bar{z}_K\}$, $K = \prod_j L_j$. Each point from \bar{Z} corresponds to a point on the uniform grid defined by $[L_1] \times \dots \times [L_{d_Z}]$, where $[L_j]$ denotes the set of L_j possible quantization values of the j dimension. Points in \bar{Z} encode particular graph substructures. We visualise our discrete latent space, defined by \bar{Z} , as the matrix of black points in Figure 2. The discrete latent representation of graph \mathcal{G} is the set $Z_G = \{z_1^q, \dots, z_n^q\}$, $z_i^q \in \bar{Z}$.

The quantization operator is permutation equivariant and so is the mapping from the initial graph \mathcal{G} to its discrete representation in the latent space as long as the ϕ graph encoder is permutation equivariant. Thus for any P permutation matrix the following equivariance relation holds:

$$P^T Z_G = \mathcal{F}(P^T Z) = \mathcal{F}(\phi(P^T E P, P^T X)) \quad (7)$$

Using an equivariant decoder $\theta(Z_G)$, which will operate on the assumption of a fully-connected graph over the node embeddings Z_G , results in reconstructed graphs that are node permutation equivariant with the original input graphs.

3.2. Learning Diffusion Bridges over the Discrete Latent Space of Graphs

We will now show how to modify the diffusion bridge processes to operate over the discrete latent space we just described. Our latent space describes graphs as a set of discrete node embeddings² and thus we need no decomposition of the score function estimations to node- and adjacency-specific score components. We use Brownian motion, $dZ_t = \sigma_t dW_t$, as the non-conditional diffusion process \mathbb{Q} . The dynamic of the x -bridge’s drift can be accordingly derived as:

$$\eta^{x=Z_G}(Z_t, t) = \sigma_t^2 \frac{Z_G - Z_t}{\beta_T - \beta_t}, \beta_t = \int_0^t \sigma_s^2 ds \quad (8)$$

where the diffusion coefficient σ_t now depends only on the time variable. Since the domain of the discrete latent space is a set we can decompose it in a node-wise manner as $\Omega = I_1 \times \dots \times I_n$, where $I_i = \bar{Z}$. As a result, the expectation simplifies to one-dimensional integrals, and the Π -bridge’s drift is:

$$\eta^\Pi(Z_t, t) = [\eta^{I_i}(Z_t^i, t)]_{i=1}^n$$

$$\eta^{I_i}(Z_t^i, t) = \sigma_t^2 \nabla_{Z_t^i} \log \sum_{k=1}^K \exp\left(-\frac{\|Z_t^i - \bar{z}_k\|^2}{2(\beta_T - \beta_t)}\right) \quad (9)$$

the straight through estimator.

²The node embeddings explicitly encode node neighborhood information as a direct result of the GNN encoding. Thus the adjacency matrix information is encoded in the node embeddings.

where $\bar{z}_k \in \bar{Z}$, K is the number of fixed points of \bar{Z} , Z_t^i is the feature of i^{th} latent node dimension of Z_t . By estimating the drift terms over the discrete set-structured latent space we eliminate the computational cost of denoising processes that operate over fully-connected graphs, which is a computational bottleneck present in most diffusion-based models for graphs.

Moreover, as a result of the steering forces the diffusion processes are guided towards the conditioning samples for the x -bridges and eventually to the data distributions for the Π -bridges for arbitrary initialisation. Consequently, these bridges allow for a flexible design of their prior distributions \mathbb{P}_0 . We experimentally verify the model performance with a fixed-point and a standard normal distribution bridge prior. We provide the proofs and discuss the training algorithms in Appendix A.1.

4. Experiments

We evaluate GLAD’s reconstruction and generation performance on generic and molecule graph problems. We compare against a number of baselines, which we characterise along two dimensions: how they do the generation, autoregressively (**A.R**) or one-shot (**O.S**), and whether they operate on the data space (**D.**) or on a latent space (**L.**).

4.1. Generic Graph Generation

We evaluate GLAD’s ability to capture underlying graph structures by experiments on three generic graph datasets: (a) Ego-small (Sen et al., 2008), (b) Community-small, and (c) Enzymes (Schomburg et al., 2004). We adopt the same train/test split as (Jo et al., 2022) for a fair comparison with their baselines. We evaluate generative performance by measuring the maximum mean discrepancy (MMD) between the generated set and test set distributions of the following graph properties: degree (**Deg.**), clustering coefficient (**Clus.**), and orbit occurrences of 4 nodes (**Orb.**) (You et al., 2018b).

Baselines and Implementation Details: Here under the one-shot approach we compare to GDSS, (Jo et al., 2022) and DiGress, (Vignac et al., 2023), which are diffusion based models that operate directly in the original graph data space, and GraphVAE (Simonovsky & Komodakis, 2018) and GNF (Liu et al., 2019) which operate over graph latent structures. Under the autoregressive baselines on the original data space we have GraphRNN, (You et al., 2018a), GraphAF (Shi et al., 2020), a flow-based model, and GraphArm, (Kong et al., 2023), an auto-regressive diffusion model, and on a latent space we have GraphDF, (Luo et al., 2021), an autoregressive flow-based model, and VQ-GAE, (Boget et al., 2023), an autoregressive model on the discrete latent space. We provide the additional details on the experiments

and the model architectures in Appendix A.2.

Results: We give the evaluation results for the generic graph generation in Table 1. GLAD exhibits quite competitive performance when compared to state-of-the-art baselines on different evaluation metrics; it consistently maintains the lowest average MMD distance across all three datasets. Moreover, GLAD significantly outperforms all models that make explicit use of latent space structures, namely GraphVAE, GNF, GraphDF, and VQ-GAE. These accomplishments highlight two pivotal strengths of our approach: first, our discrete latent space is able to encode rich local graph structures, serving as a cornerstone for any latent-driven graph generative models. Second, our diffusion bridge model works seamlessly within the proposed discrete latent space, which is underscored by its capability to capture the set-based latent representation of graphs. While our model does not operate directly on the data space of graphs like other diffusion frameworks such as GDSS and DiGress, it has demonstrated the superior performance to understand the underlying topologies of graphs in a holistic manner.

4.2. Molecule Graph Generation

Here we want to evaluate the capacity of GLAD to capture the complex dependencies between atoms and bonds as they appear in different molecules. We conduct experiments on two standard datasets: QM9 (Ramakrishnan et al., 2014) and ZINC250k (Irwin et al., 2012). Following (Jo et al., 2022), we remove hydrogen atoms and kekulize molecules by RDKit Landrum et al. (2016). We quantitatively evaluate all methods in terms of validity without any post-hoc corrections (**Val.**), uniqueness (**Uni.**), and novelty (**Nov.**) of 10000 molecules generated by each of them. We also compute two more salient metrics which quantify how well the distribution of the generated graphs aligns with the real data distribution, namely Fréchet ChemNet Distance (**FCD**) and Neighborhood Subgraph Pairwise Distance Kernel (**NSPDK**) MMD. FCD evaluates the distance in the chemical space between generated and training graphs by using the activation of the ChemNet’s penultimate layer, while NSPDK measures the MMD distance, showing the similarity of underlying structures between generated and test molecules, which typically considers both the atom and bond types in computation. More details on the experimental setup is provided in Appendix A.2.

Baseline Details: The one-shot baselines that operate on the data space are: MoFlow, (Zang & Wang, 2020), a conditional flow-based model; GDSS, DiGress, and EDP-GNN, (Niu et al., 2020), a continuous score-based model. The autoregressive baselines are GraphAF, GraphArm, GraphDF, and VQ-GAE.

Results: We give the evaluation results for the molecule generation in Table 2. GLAD is the first one-shot model

Table 1. **Generation results on the generic graph datasets.** We show the mean values of 15 runs for each experiment, where lower results indicate better performance. The baselines are sourced from (Jo et al., 2022; Kong et al., 2023). We use the abbreviations O.S, A.R, L., D. to stand for one-shot, auto-regressive, latent space, and data space, respectively. Hyphen (-) denotes unreproducible results. The 1st and 2nd best results are bolded and underlined, respectively. We further provide standard deviations and inference time in Appendix.

		COMMUNITY-SMALL				EGO-SMALL				ENZYMES				
		Deg.	Clus.	Orb.	Avg.	Deg.	Clus.	Orb.	Avg.	Deg.	Clus.	Orb.	Avg.	
A.R.	D.	GraphAF	0.180	0.200	0.020	<u>0.133</u>	0.030	0.110	0.001	0.047	1.669	1.283	0.266	1.073
		GraphRNN	0.080	0.120	0.040	0.080	0.090	0.220	0.003	0.104	0.017	0.062	0.046	0.042
		GraphArm	0.034	0.082	0.004	0.040	0.019	<u>0.017</u>	0.010	0.015	0.029	0.054	0.015	0.033
	L.	GraphDF	0.060	0.120	0.030	<u>0.070</u>	0.040	0.130	0.010	<u>0.060</u>	1.503	1.061	0.202	0.922
		VQ-GAE	<u>0.032</u>	0.062	<u>0.005</u>	<u>0.033</u>	0.021	0.041	0.007	0.023	-	-	-	-
O.S.	D.	GDSS	0.045	0.086	0.007	<u>0.046</u>	0.021	0.024	0.007	0.017	0.026	0.061	0.009	0.032
		DiGress	0.047	0.041	0.026	0.038	0.015	0.029	0.005	0.016	0.004	0.083	<u>0.002</u>	0.030
	L.	GraphVAE	0.350	0.980	0.054	<u>0.623</u>	0.130	0.170	0.050	0.117	1.369	0.629	0.191	0.730
		GNF	0.200	0.200	0.110	0.170	0.030	0.100	0.001	0.044	-	-	-	-
		GLAD	0.027	<u>0.044</u>	0.006	0.026	0.012	0.013	0.004	0.010	<u>0.012</u>	0.014	0.001	0.009

Table 2. **Generation results on the molecule datasets.** We show the mean values of 3 runs for each experiment. The baselines are sourced from (Jo et al., 2022; Kong et al., 2023). We use the abbreviations O.S, A.R, L., D. to stand for one-shot, auto-regressive, latent space, and data space, respectively. The 1st and 2nd best results are bolded and underlined, respectively. We further provide standard deviations and inference time in Appendix.

		QM9					ZINC250k					
		Val. \uparrow	Uni. \uparrow	Nov. \uparrow	NSPDK \downarrow	FCD \downarrow	Val. \uparrow	Uni. \uparrow	Nov. \uparrow	NSPDK \downarrow	FCD \downarrow	
A.R.	D.	GraphAF	74.43	88.64	86.59	0.020	5.27	68.47	98.64	100	0.044	16.02
		GraphArm	90.25	95.62	70.39	0.002	1.22	88.23	99.46	100	0.055	16.26
	L.	GraphDF	93.88	98.58	98.54	0.064	10.93	90.61	99.63	100	0.177	33.55
		VQ-GAE	88.00	97.23	78.12	0.0023	0.8	65.7	99.96	99.97	0.008	5.4
O.S.	D.	EDP-GNN	47.52	99.25	86.58	0.005	2.68	82.97	99.79	100	0.049	16.74
		GDSS	95.72	98.46	86.27	0.003	2.90	97.01	99.64	100	0.019	14.66
		DiGress	99.0	96.66	33.40	<u>0.0005</u>	0.360	<u>91.02</u>	81.23	100	0.082	23.06
		MoFlow	91.36	98.65	94.72	0.017	4.47	63.11	99.99	100	0.046	20.93
	L.	GLAD	<u>97.24</u>	97.68	39.54	0.0003	0.222	81.22	100	100	0.002	2.54

Prior	QM9				
	Val. \uparrow	Uni. \uparrow	Nov. \uparrow	NSPDK \downarrow	FCD \downarrow
$\mathcal{N}(\mathbf{0}, \mathbf{1})$	95.38	97.38	41.54	0.0004	0.330
$\mathbf{0}$	97.24	97.68	39.54	0.0003	0.222
$\mathbf{0}^\dagger$	83.12	97.54	62.44	0.0009	1.207

Table 3. **The effects of prior \mathbb{P}_0 and quantization \mathcal{F} .** Generation results on QM9 where the prior distribution is initialized as a standard normal distribution and a Dirac Δ distribution on the fixed point $\mathbf{0}$, the latter with and without quantization, denoted respectively by $\mathbf{0}$ and $\mathbf{0}^\dagger$.

that learns to generate molecular structures from a discrete latent space. Even though our model does not predict directly atom- and bond-type structures it can still generate molecules with very good validity scores with no need for

any post-hoc corrections. More importantly, it achieves state of the art performance on the two most salient metrics NSPDK and FCD that capture how well the generated distribution matches the training distribution, consistently outperforming by significant margins all baselines. We provide examples of generated molecules in Appendix A.3. GLAD can capture well both structural and chemical properties of molecules. This is achieved through our quantized latent space, which offers a suitable discrete structure to encode those properties. Furthermore, our bridge model accurately learns underlying latent molecular structures, and generates new molecules that are close to training distributions.

4.3. Ablation Studies

We will ablate two dimensions within the overall GLAD method: different design choices on the latent space, and

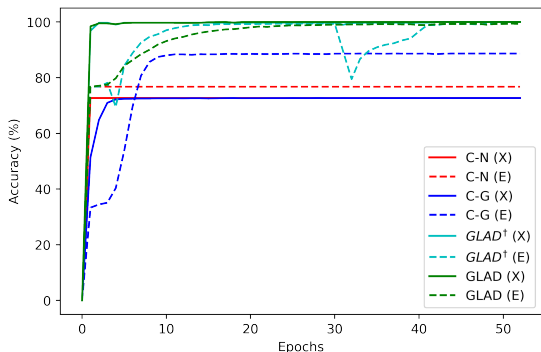


Figure 3. Test reconstruction performance of different latent spaces on QM9 dataset. Node (X) and edge (E) reconstruction accuracies. i) continuous-graph latent representation (C-G). ii) continuous-node latent representation (C-N) iii) unquantised discrete-node latent space $GLAD^\dagger$, iv) quantised discrete-node latent space GLAD.

the sensitivity of the method with different priors in the diffusion bridge processes.

Latent spaces for graphs. We claim that the discrete structure of the graph latent space is central to the success of GLAD. In order to verify that we will compare the latent space of GLAD to the following three latent spaces and generative models: i) a continuous-graph latent space where a graph \mathcal{G} is represented as $z_{\mathcal{G}} \sim q_{\phi}(z_{\mathcal{G}}|\mathcal{G})$, with $z_{\mathcal{G}} = \oplus(Z)$ and $q_{\phi}(z_{\mathcal{G}}|\mathcal{G})$ KL diverged to the standard normal ii) a continuous-node latent space where the graph representation is $z_{\mathcal{G}} \sim q_{\phi}(Z|\mathcal{G}) = \prod_i q_{\phi}(z_i|\mathcal{G})$, with $q_{\phi}(z_i|\mathcal{G})$ KL diverged to the standard normal, both i) and ii) encode graphs as continuous distributions, with support everywhere in the embedding space, and are trained with the ELBO objective. Finally in iii) we have the same embedding latent space as in ii) but a graph is not anymore a distribution, but simply Z the set of its node embeddings. The generative model in iii) is the continuous diffusion bridge; overall iii) is the unquantised latent space of GLAD, and we denote it as $GLAD^\dagger$. Even though in iii) we embed on a continuous space, as a result of the graph nature we are not covering this space, we are rather embedding in a discrete and countable subspace of it. We evaluate the quality of the underlying graph latent spaces using their bond-type (X) and atom-type (E) reconstruction accuracies on QM9, Figure 3.

The two continuous latent spaces in i) and ii) have considerably lower reconstruction accuracies compared to the two GLAD variants which preserve to a different extent the original discrete topology. Both GLAD variants converge very fast to almost 100% reconstruction accuracies. GLAD has a small advantage when it comes to the bond-type reconstructions for which its training is more stable than that of

its unquantised sibling $GLAD^\dagger$. The latent spaces of i) and ii) suffer from the so-called node-collapse problem. They are not able to well describe different atom local structures. As a result, most reconstructed nodes are assigned to the dominant Carbon atom which corresponds to roughly the 70% of all atoms in QM9.

While the two GLAD variants have a rather similar reconstruction performance this is not the case when we compare their generation performance; we train two variants with a fixed point prior (more details in the following ablation) and give the generation results in Table 3. There we see that diffusion bridges can not capture well the graph distribution when they operate in the unquantised space, with a performance drop for most measures (more importantly for the two measures capturing distribution differences, NSPDK and FCD), showing the benefits of the quantised discrete latent space. The latent spaces of the two GLAD variants are both discrete and are embedded within the same continuous space. Quantization acts as a spatial regulariser over the non-quantised discrete space by constructing a uniform grid to which the latent node embeddings are assigned instead of letting them free.

Latent Diffusion Bridge Priors: Here we evaluate generative performance with different priors; a fixed point prior $\mathbb{P}_0 = \mathbf{0}$, which is typically the central point of our discrete latent space, and a standard normal distribution prior, $\mathbb{P}_0 = \mathcal{N}(\mathbf{0}, \mathbf{I})$. We conduct the experiments on QM9 and give the results in Table 3. As a result of the steering forces of the bridge processes there are only negligible differences between the two priors making prior selection less of a nuance. With the fixed prior, we obtain generated molecules with higher validity scores, closer to the training distribution in both chemical space (FCD score), structural space (NSPDK score). Using the normal prior we have better performance in terms of uniqueness and novel novelty.

5. Conclusions

We presented GLAD a graph generative model that operates over a discrete latent space. We carefully designed that space to satisfy a number of desiderata that stem from the nature of the graph structures, namely it should allow for graph invariant distribution modelling, it should have rich representational power, and it should respect the inherently discrete nature of graphs. To learn generative models over that space we leveraged diffusion bridges which we adapted to our discrete latent space by appropriately adjusting their drift terms. We empirically validate GLAD on a number of benchmarks and show that it achieves state of the art generative performance, surpassing other baselines independently of whether they operate on the original or on latent spaces. We systematically ablated different design choices for graph latent space representation and show that our discrete latent

space brings clear performance advantages over continuous alternatives both in terms of reconstruction as well as generation. This paves the way for a more systematic exploration of graph generative modelling in latent spaces, something that until now has received rather limited attention.

Impact

The paper presents a generative model for graphs. Such methods find applicability in settings such as chemical compound design, protein and drug design, with a significant potential for positive societal contributions if successful. At the same time they could also be used by malign actors for the design of harmful chemical, biological and other types of agents. However, the actual transfer of the results of such models to the lab and from there to production, requires significant resources, which creates a first safeguard against their malicious use. In addition there are international treaties that have established strict safeguards when it comes in the manufacturing of harmful agents.

References

- Albert, R. and Barabási, A.-L. Statistical mechanics of complex networks. *Reviews of modern physics*, 74(1):47, 2002.
- Bengio, Y., Léonard, N., and Courville, A. Estimating or propagating gradients through stochastic neurons for conditional computation. *arXiv preprint arXiv:1308.3432*, 2013.
- Boget, Y., Gregorova, M., and Kalousis, A. Vector-quantized graph auto-encoder. *arXiv preprint arXiv:2306.07735*, 2023.
- Chen, X., Han, X., Hu, J., Ruiz, F., and Liu, L. Order matters: Probabilistic modeling of node sequence for graph generation. In Meila, M. and Zhang, T. (eds.), *Proceedings of the 38th International Conference on Machine Learning*, volume 139 of *Proceedings of Machine Learning Research*, pp. 1630–1639. PMLR, 18–24 Jul 2021.
- Doob, J. L. and Doob, J. *Classical potential theory and its probabilistic counterpart*, volume 262. Springer, 1984.
- Erdős, P., Rényi, A., et al. On the evolution of random graphs. *Publ. math. inst. hung. acad. sci.*, 5(1):17–60, 1960.
- Heng, J., De Bortoli, V., Doucet, A., and Thornton, J. Simulating diffusion bridges with score matching. *arXiv preprint arXiv:2111.07243*, 2021.
- Irwin, J. J., Sterling, T., Mysinger, M. M., Bolstad, E. S., and Coleman, R. G. Zinc: a free tool to discover chemistry for biology. *Journal of chemical information and modeling*, 52(7):1757–1768, 2012.
- Jin, W., Barzilay, R., and Jaakkola, T. Junction tree variational autoencoder for molecular graph generation. In *International conference on machine learning*, pp. 2323–2332. PMLR, 2018.
- Jo, J., Lee, S., and Hwang, S. J. Score-based generative modeling of graphs via the system of stochastic differential equations. In *International Conference on Machine Learning*, pp. 10362–10383. PMLR, 2022.
- Kingma, D. P. and Welling, M. Auto-encoding variational bayes. *arXiv preprint arXiv:1312.6114*, 2013.
- Kong, L., Cui, J., Sun, H., Zhuang, Y., Prakash, B. A., and Zhang, C. Autoregressive diffusion model for graph generation. In *International Conference on Machine Learning*, pp. 17391–17408. PMLR, 2023.
- Landrum, G. et al. Rdkit: Open-source cheminformatics software, 2016. URL <http://www.rdkit.org/>, <https://github.com/rdkit/rdkit>, 149(150):650, 2016.
- Lejay, A. The girsanov theorem without (so much) stochastic analysis. *Séminaire de Probabilités XLIX*, pp. 329–361, 2018.
- Liu, J., Kumar, A., Ba, J., Kiros, J., and Swersky, K. Graph normalizing flows. *Advances in Neural Information Processing Systems*, 32, 2019.
- Liu, Q., Allamanis, M., Brockschmidt, M., and Gaunt, A. Constrained graph variational autoencoders for molecule design. *Advances in neural information processing systems*, 31, 2018.
- Liu, X., Wu, L., Ye, M., and qiang liu. Learning diffusion bridges on constrained domains. In *The Eleventh International Conference on Learning Representations*, 2023.
- Luo, Y., Yan, K., and Ji, S. Graphdf: A discrete flow model for molecular graph generation. In *International Conference on Machine Learning*, pp. 7192–7203. PMLR, 2021.
- Mentzer, F., Minnen, D., Agustsson, E., and Tschannen, M. Finite scalar quantization: Vq-vae made simple. *arXiv preprint arXiv:2309.15505*, 2023.
- Niu, C., Song, Y., Song, J., Zhao, S., Grover, A., and Ermon, S. Permutation invariant graph generation via score-based generative modeling. In *International Conference on Artificial Intelligence and Statistics*, pp. 4474–4484. PMLR, 2020.

- Oksendal, B. *Stochastic differential equations: an introduction with applications*. Springer Science & Business Media, 2013.
- Peluchetti, S. Non-denoising forward-time diffusions, 2022. URL <https://openreview.net/forum?id=oVfIKuhqfC>.
- Ramakrishnan, R., Dral, P. O., Rupp, M., and Von Lilienfeld, O. A. Quantum chemistry structures and properties of 134 kilo molecules. *Scientific data*, 1(1):1–7, 2014.
- Samanta, B., De, A., Jana, G., Gómez, V., Chattaraj, P., Ganguly, N., and Gomez-Rodriguez, M. Nevae: A deep generative model for molecular graphs. *Journal of machine learning research*, 21(114):1–33, 2020.
- Schomburg, I., Chang, A., Ebeling, C., Gremse, M., Heldt, C., Huhn, G., and Schomburg, D. Brenda, the enzyme database: updates and major new developments. *Nucleic acids research*, 32(suppl_1):D431–D433, 2004.
- Sen, P., Namata, G., Bilgic, M., Getoor, L., Galligher, B., and Eliassi-Rad, T. Collective classification in network data. *AI magazine*, 29(3):93–93, 2008.
- Shi, C., Xu, M., Zhu, Z., Zhang, W., Zhang, M., and Tang, J. Graphaf: a flow-based autoregressive model for molecular graph generation. *arXiv preprint arXiv:2001.09382*, 2020.
- Simonovsky, M. and Komodakis, N. Graphvae: Towards generation of small graphs using variational autoencoders. In *Artificial Neural Networks and Machine Learning—ICANN 2018: 27th International Conference on Artificial Neural Networks, Rhodes, Greece, October 4-7, 2018, Proceedings, Part I 27*, pp. 412–422. Springer, 2018.
- Vignac, C., Krawczuk, I., Siraudin, A., Wang, B., Cevher, V., and Frossard, P. Digress: Discrete denoising diffusion for graph generation. In *The Eleventh International Conference on Learning Representations*, 2023.
- Wang, H., Wang, J., Wang, J., Zhao, M., Zhang, W., Zhang, F., Xie, X., and Guo, M. Graphgan: Graph representation learning with generative adversarial nets. In *Proceedings of the AAAI conference on artificial intelligence*, 2018.
- You, J., Ying, R., Ren, X., Hamilton, W., and Leskovec, J. Graphrnn: Generating realistic graphs with deep autoregressive models. In *International conference on machine learning*, pp. 5708–5717. PMLR, 2018a.
- You, J., Ying, R., Ren, X., Hamilton, W., and Leskovec, J. Graphrnn: Generating realistic graphs with deep autoregressive models. In *International conference on machine learning*, pp. 5708–5717. PMLR, 2018b.
- Zang, C. and Wang, F. Moflow: an invertible flow model for generating molecular graphs. In *Proceedings of the 26th ACM SIGKDD international conference on knowledge discovery & data mining*, pp. 617–626, 2020.

A. Appendix.

In the appendix we present additional details of the paper. We give in Section A.1 the training procedure, in Section A.2 the experimental details, and provide generated molecule examples in Section A.3.

A.1. Training

We train GLAD with a two-stage procedure. We first train a graph autoencoder and then learn the graph latent diffusion bridge over the quantised discrete space defined on the graph autoencoder output.

In the first stage, we train the graph-autoencoder, which learns a structural mapping from the graph data space to the designed latent space and reconstructs original graphs from their latent representations. As a technical detail, we note that the rounding operator \mathcal{R} of the quantization is non-differentiable. To ensure end-to-end training of our discrete graph latent space mapping, we use the straight-through estimator (STE) (Bengio et al., 2013), implemented with a stop-gradient operator \mathcal{S} as $Z_{\mathcal{G}} \mapsto Z + \mathcal{S}(Z_{\mathcal{G}} - Z)$. In addition, we use mean-squared loss as it offers more stable training experiments. Our graph autoencoder training is described in Algorithm 1.

Algorithm 1 Graph AutoEncoder Training Algorithm

- 1: **Input:** Encoder ϕ , decoder θ , the number of quantization levels per dimension L_j .
 - 2: **for** # training iterations **do**
 - 3: Sample a minibatch $\mathcal{G} = (\mathbf{X}, \mathbf{E})$
 - 4: Encode to latent nodes $\mathbf{Z} \leftarrow \phi(\mathcal{G})$
 - 5: Quantise $\mathbf{Z}_{\mathcal{G}} \leftarrow \mathcal{F}(\mathbf{Z}, L_j)$ {Equation 6}
 - 6: Straight-through estimator $\mathbf{Z}_{\mathcal{G}} \mapsto \mathbf{Z} + \text{stop-gradient}(\mathbf{Z}_{\mathcal{G}} - \mathbf{Z})$
 - 7: Decode $\bar{\mathcal{G}} = (\bar{\mathbf{X}}, \bar{\mathbf{E}}) \leftarrow \theta(\mathbf{Z}_{\mathcal{G}})$
 - 8: Compute MSE $\mathcal{L} \leftarrow \|\mathbf{X} - \bar{\mathbf{X}}\|^2 + \|\mathbf{E} - \bar{\mathbf{E}}\|^2$
 - 9: Update the models ϕ, θ by gradient descent w.r.t. their parameters $\nabla_{\phi, \theta} \mathcal{L}$
 - 10: **end for**
-

In the second stage, we freeze the trained graph-autoencoder parameters, and train our generative component—namely the drift model. We adjust the derivations of Liu et al. (2023) to the graph setting. We use Brownian motion as the non-conditional diffusion process in Equation 1:

$$\mathbb{Q} : dZ_t = \sigma_t dW_t, \quad \beta_t = \int_0^t \sigma_s^2 ds \quad (10)$$

The transition probability between states follows a Gaussian distribution, whose density is defined as $q_{T|t}(Z_T|Z_t) = \mathcal{N}(Z_T; Z_t, \beta_T - \beta_t)$. Replacing this density to the transition probability density in Equation 2, we get the x -bridge drift:

$$\begin{aligned} \eta^{x=Z_{\mathcal{G}}}(Z_t, t) &= \eta(Z_t, t) + \sigma_t^2 \nabla_{Z_t} \log q_{T|t}(Z_{\mathcal{G}}|Z_t) \\ &= 0 + \sigma_t^2 \frac{Z_{\mathcal{G}} - Z_t}{\beta_T - \beta_t} \\ &= \sigma_t^2 \frac{Z_{\mathcal{G}} - Z_t}{\beta_T - \beta_t} \end{aligned} \quad (11)$$

Thus, the governing law of the x -bridge is:

$$\mathbb{Q}^{x=Z_{\mathcal{G}}} : dZ_t = \sigma_t^2 \frac{Z_{\mathcal{G}} - Z_t}{\beta_T - \beta_t} dt + \sigma_t dW_t \quad (12)$$

We sample from the $t \in [0, T]$ time step of the x -bridge as follows:

$$Z_t = \frac{\beta_t}{\beta_T} (Z_{\mathcal{G}} + (\beta_T - \beta_t) Z_0) + \xi \sqrt{\beta_t \left(1 - \frac{\beta_t}{\beta_T}\right)}, \quad \xi \sim \mathcal{N}(0, I) \quad (13)$$

By plugging the transition probability $q_{T|t}(Z_T|Z_t)$ into Equation 3, we obtain the Π -bridge drift:

$$\begin{aligned}\eta^\Pi(Z_t, t) &= \eta(Z_t, t) + \sigma_t^2 \mathbb{E}_{Z_G \sim q_{T|t, \Omega}} [\nabla_{Z_t} \log q_{T|t}(Z_G|Z_t)] \\ &= 0 + \sigma_t^2 \mathbb{E}_{Z_G \sim q_{T|t, \Omega}} \left[\frac{Z_G - Z_t}{\beta_T - \beta_t} \right] \\ &= \sigma_t^2 \mathbb{E}_{Z_G \sim q_{T|t, \Omega}} \left[\frac{Z_G - Z_t}{\beta_T - \beta_t} \right]\end{aligned}\quad (14)$$

where $q_{T|t, \Omega}$ is the Ω -truncated transition probability density function. When \mathbb{Q} is Brownian motion its Ω -truncated transition probability density is a truncated Gaussian density given by $q_{T|t, \Omega}(Z_G|Z_t) \propto \mathbb{I}(Z_G \in \Omega) q_{T|t}(Z_G|Z_t)$.

We observe that the truncated transition density considers the existing elements Z_G of the discrete domain Ω . However, our graph latent representation is a set-based structure, the discrete domain Ω can thus be factorized over latent node dimension, denoted as $\Omega = I_1 \times \dots \times I_n$, with $I_i = \bar{Z}$ in Section 3.1. Intuitively, this factorization represents for independent conditional stochastic processes over each latent node dimension of the given graph latent structure. Hence, the Π -bridge's drift can be decomposed as:

$$\begin{aligned}\eta^\Pi(Z_t, t) &= [\eta^{I_i}(Z_t^i, t)]_{i=1}^n \\ \text{where } \eta^{I_i}(Z_t^i, t) &= \sigma_t^2 \mathbb{E}_{\bar{z}_k \sim q_{T|t, \bar{Z}}} \left[\frac{\bar{z}_k - Z_t^i}{\beta_T - \beta_t} \right]\end{aligned}\quad (15)$$

The expectation is now taken over the truncated transition probability along each latent node dimension I_i , whose density can be represented as following:

$$\begin{aligned}q_{T|t, \bar{Z}}(\bar{z}_k) &\propto \mathbb{I}(\bar{z}_k \in \bar{Z}) \frac{q_{T|t}(\bar{z}_k|Z_t^i)}{\sum_{j=1}^K q_{T|t}(\bar{z}_j|Z_t^i)} \\ \text{where the density } q_{T|t}(\bar{z}_j|Z_t^i) &\text{ is } \mathcal{N}(\bar{z}_j; Z_t^i, \beta_T - \beta_t)\end{aligned}\quad (16)$$

The Π -bridge's drift along each latent node dimension can be written in a closed-form solution:

$$\begin{aligned}\eta^{I_i}(Z_t^i, t) &= \sigma_t^2 \mathbb{E}_{\bar{z}_k \sim q_{T|t, \bar{Z}}} \left[\frac{\bar{z}_k - Z_t^i}{\beta_T - \beta_t} \right] \\ &= \sigma_t^2 \sum_{k=1}^K \frac{q_{T|t}(\bar{z}_k|Z_t^i)}{\sum_{j=1}^K q_{T|t}(\bar{z}_j|Z_t^i)} \frac{\bar{z}_k - Z_t^i}{\beta_T - \beta_t} \\ &= \sigma_t^2 \sum_{k=1}^K \frac{\exp\left(-\frac{\|Z_t^i - \bar{z}_k\|^2}{2(\beta_T - \beta_t)}\right)}{\sum_{j=1}^K \exp\left(-\frac{\|Z_t^i - \bar{z}_j\|^2}{2(\beta_T - \beta_t)}\right)} \frac{\bar{z}_k - Z_t^i}{\beta_T - \beta_t} \\ &= \sigma_t^2 \nabla_{Z_t^i} \log \sum_{k=1}^K \exp\left(-\frac{\|Z_t^i - \bar{z}_k\|^2}{2(\beta_T - \beta_t)}\right)\end{aligned}\quad (17)$$

For the completeness of the presentation, we show the original proof of the training objective in a more explicit way to our case. Given that, we need to minimize the Kullback-Leibler divergence between the two probability path measures $\min_{\psi} \{\mathcal{L}(\psi) := \mathcal{KL}(\mathbb{Q}^\Pi \| \mathbb{P}^\psi)\}$ in Section 2.2, Π is our discrete latent distribution of graphs. Following (Liu et al., 2023), the KL objective is proved to be equivalent to:

$$\mathcal{KL}(\mathbb{Q}^\Pi \| \mathbb{P}^\psi) = \mathbb{E}_{Z_G \sim \Pi} [\mathcal{KL}(\mathbb{Q}^{x=Z_G} \| \mathbb{P}^\psi)] + \text{const.}\quad (18)$$

By Girsanov theorem (Lejay, 2018), this objective can be further decomposed as following:

$$\mathcal{L}(\psi) = \mathbb{E}_{Z_G \sim \Pi, Z_t \sim \mathbb{Q}^{x=Z_G}} \left[-\log p_0(Z_0) + \frac{1}{2} \int_0^T \left\| \sigma_t^{-1} (\eta^\psi(Z_t, t) - \eta^{x=Z_G}) \right\|^2 \right] + \text{const.} \quad (19)$$

In our experiments, the prior distribution $\log p_0(Z_0)$ is a Dirac Δ distribution on the fixed point $\mathbf{0}$, the central mass of the quantized space, thus $\log p_0(Z_0)$ is constant. Applying the definition of $\eta^\psi(Z_t, t)$ in Section 2.2 to Equation 19, our final training objective can be obtained with a closed-form solution:

$$\mathcal{L}(\psi) = \mathbb{E}_{t \sim [0, T], Z_G \sim \Pi, Z_t \sim \mathbb{Q}^{x=Z_G}} \left[\left\| f_\psi(Z_t, t) - \sigma_t^{-1} (\eta^{x=Z_G}(Z_t, t) - \eta^\Pi(Z_t, t)) \right\|^2 \right] + \text{const} \quad (20)$$

At the sampling of new data, we apply the Euler–Maruyama discretization scheme on the model bridge \mathbb{P}^ψ that gives:

$$Z_{t+1} = Z_t + (\sigma_t f_\psi(Z_t, t) + \eta^\Pi(Z_t, t)) \delta_t + \sigma_t \sqrt{\delta_t} \xi, \quad \xi \sim \mathcal{N}(0, I), \quad Z_0 \sim \mathbb{P}_0 \quad (21)$$

where δ_t is the discretization step. Our graph generative component training is shown in Algorithm 2.

Algorithm 2 Graph Latent Diffusion Bridge Training Algorithm.

- 1: **Input:** The trained graph autoencoder ϕ, θ , the number of quantization levels per dimension L_j , the drift model f_ψ , the number of diffusion steps T , the diffusion coefficient scheduler σ_s , the prior distribution \mathbb{P}_0 .
 - 2: **for** # training iterations **do**
 - 3: Sample a minibatch $\mathcal{G} = (\mathbf{X}, \mathbf{E})$, a time steps vector $t \in [0, T]$, a noise vector $\xi \sim \mathcal{N}(0, I)$, and $\mathbf{Z}_0 \sim \mathbb{P}_0$
 - 4: Encode to latent nodes $\mathbf{Z} \leftarrow \phi(\mathcal{G})$
 - 5: Quantise $\mathbf{Z}_G \leftarrow \mathcal{F}(\mathbf{Z}, L_j)$
 - 6: Sample from the x -bridge $\mathbf{Z}_t \leftarrow \frac{\beta_t}{\beta_T} (\mathbf{Z}_G + (\beta_T - \beta_t) \mathbf{Z}_0) + \xi \sqrt{\beta_t \left(1 - \frac{\beta_t}{\beta_T}\right)}$
 - 7: Initialize the node-wise objective list $\bar{\eta} \leftarrow []$
 - 8: **for** each latent node dimension I_i **in** Ω **do**
 - 9: Compute the x -bridge’s drift $\eta^x \leftarrow \sigma_t^2 \frac{\mathbf{Z}_G^{I_i} - \mathbf{Z}_t^{I_i}}{\beta_T - \beta_t}$ {Equation 8}
 - 10: Compute the Π -bridge’s drift $\eta^\Pi \leftarrow \sigma_t^2 \nabla_{\mathbf{Z}_t^{I_i}} \log \sum_{k=1}^K \exp\left(-\frac{\|\mathbf{Z}_t^{I_i} - \bar{z}_k\|^2}{2(\beta_T - \beta_t)}\right)$, $\bar{z}_k \in \bar{Z}$ {Equation 9}
 - 11: Compute the current node objective $\bar{\eta}^{I_i} \leftarrow \sigma^{-1}_t (\eta^x - \eta^\Pi)$
 - 12: Append to the objective list $\bar{\eta} \leftarrow [\bar{\eta}, \bar{\eta}^{I_i}]$
 - 13: **end for**
 - 14: Compute MSE $\mathcal{L} \leftarrow \|f_\psi(\mathbf{Z}_t, t) - \bar{\eta}\|^2$. {Equation 5}
 - 15: Update the drift model f_ψ by gradient descent w.r.t its parameters $\nabla_\psi \mathcal{L}$
 - 16: **end for**
-

A.2. Experiments

A.2.1. MODEL ARCHITECTURES

In our research problem, we process data that lie on both graph- and set-based structures. We opt to employ a general-purpose architecture such as transformers. Future works could consider a more specific choice of architectures especially designed for graphs or sets. We utilize the graph transformer (Vignac et al., 2023) and further customize the architecture to adapt to the encoder ϕ , the decoder θ , and the drift model f_ψ . Typically, the graph transformer takes a node feature matrix $X \in \mathbb{R}^{n \times d_X}$, an edge feature matrix $E \in \mathbb{R}^{n \times n \times d_E}$, and a global feature vector $Y \in \mathbb{R}^{d_Y}$ as inputs. For the encoder, we incorporate a second-order adjacency matrix (Jo et al., 2022) to model long-range dependencies. Due to the inherent limitations of most GNNs, we compute structural features like cycle counts and spectral features of the graph-Laplacian decomposition as hand-crafted input features. The decoder and drift model take a set-based data structure as input. Moreover, sets are

Table 4. **Generic graph statistics** on three benchmark datasets: community small, ego small, and enzymes.

	Number of Graphs	Number of Nodes	Real / Synthetic
COMMUNITY-SMALL	100	$12 \leq X \leq 20$	Synthetic
EGO-SMALL	200	$4 \leq X \leq 18$	Real
ENZYMES	587	$10 \leq X \leq 125$	Real

more or less considered as fully-connected graphs. Hence, we use augmented edge matrices that enable to adapt the main architecture design. These augmented matrices are simply defined as a pairwise latent node distance matrix:

$$E^+ = Z \times Z^T \quad (22)$$

Here, $Z \in \mathbb{R}^{n \times d_z}$ represents a latent node representation matrix. Specifically, Z is equal to Z_G for the decoder, and Z is equal to Z_t for the drift model. In addition, we use pooled node features $Y = \oplus(Z)$ as global features for the decoder and drift model.

A.2.2. QUANTIZATION

We empirically find that a quantized latent space of dimension $d_z = 6$ works well to encode graphs within low reconstruction errors. In all experiments, we fix the quantization vector $L = [5, 5, 5, 5, 5, 5]$ where at each latent node dimension L_j , $1 \leq j \leq 6$, we quantize to one of five possible values $[-2, -1, 0, 1, 2]$. In total, we have $K = 5^6$ quantization points that are uniformly distributed in the discrete latent space. These points serve as the referent points to which latent nodes are assigned. For illustration, given a raw latent node vector Z^i , its quantized version Z_q^i is obtained as following:

$$Z^i = \begin{bmatrix} -1.1 \\ -1.7 \\ -0.01 \\ 0.1 \\ 3.2 \\ 0.6 \end{bmatrix} \rightarrow \frac{L_j}{2} \tanh Z_j^i \rightarrow \begin{bmatrix} -2.00 \\ -2.34 \\ -0.03 \\ 0.25 \\ 2.49 \\ 1.34 \end{bmatrix} \rightarrow \text{Rounding} \rightarrow Z_q^i = \begin{bmatrix} -2 \\ -2 \\ 0 \\ 0 \\ 2 \\ 1 \end{bmatrix}$$

The same principle is applied to all latent nodes. Moreover, we visualize the distribution of number latent nodes per quantization point in Figure 6. We observe that there is a good matching between the train and test distributions.

A.2.3. EXPERIMENTAL DETAILS

We provide the hyperparameter details in the main experiments in Table 8.

Diffusion noise scheduler: We set to the diffusion coefficient to an exponential process $\sigma_t^2 = \sigma_{\min} * \sigma_{\max} \exp(-\sigma_{\max} * t)$ where we fix $\sigma_{\min} = 1$ and conduct an ablation study on $\sigma_{\max} = \{1, 3, 7\}$.

Generic graph generation task: We provide the statistics of three generic graph datasets in Table 4. We adopt the same train/test split as (Jo et al., 2022) for a fair comparison with their baselines. In each experiment, we report the means and standard deviations of 15 runs. We do not include the enzyme baselines of VQ-GAE and GNF due to the absence open-source codes or time training constraints. On the generic graphs, there are no explicit information about nodes available for training. Therefore, we use node degrees as augmented node features in GLAD. Each graph is represented by a node feature matrix $X \in \{0, 1\}^{n \times d_x}$ and an edge feature matrix $E \in \{0, 1\}^{n \times n}$, where d_x corresponds to the number of possible node degrees. During the generation step, we apply the rounding operator after the sigmoid function to reconstruct the original edges. We empirically find that the rounding operator works well for the edge reconstruction. Similarly, on the diffusion bridges, we round the values of the terminal state Z_T to the nearest integers. We apply an exponential learning rate scheduler (with a constant learning rate decay of 0.999) and a cosine anneal learning scheduler when training the graph autoencoder and the drift model, respectively. We use the Pytorch automatic differentiation package to compute the

Table 5. Molecule graph statistics on QM9 and ZINC250k.

	Number of Graphs	Number of Nodes	Number of Node Types	Number of Edge Types
QM9	133885	$1 \leq X \leq 9$	4	3
ZINC250k	249455	$6 \leq X \leq 38$	9	3

Π -bridge’s drift derivative in Equation 9. We conduct an ablation study on architecture sizes with different number of layers $\{4, 6, 8\}$, hidden node features $\{64, 128, 256\}$, and hidden edge features $\{32, 64, 128\}$. We choose the best checkpoint that has the lowest average MMD distance for comparing with the baselines. In each evaluation, we generate an equal number of graphs to the test set. Follow Jo et al. (2022), we use the Gaussian Earth Mover’s Distance (EMD) kernel to calculate MMD thanks to its computational stability. Our detailed results are reported in Table 6.

Molecule graph generation task: We provide the statistics of the molecule graph datasets in Table 7. Following the procedure outlined in (Jo et al., 2022), we kekulize the molecules by the RDKit library (Landrum et al., 2016) and remove hydrogen atoms. The input graph is represented by a node feature matrix $X \in \{0, 1\}^{n \times d_X}$, and a scaled edge feature matrix $\{0, 1/3, 2/3, 1\}^{n \times n}$, where d_X is the number of possible atom types. During the generation step, we un-scale edge predictions back to $[0, 3]$, then round them to the nearest integers. In addition, we apply the rounding operator to the latent diffusion bridges at the terminal state Z_T . Similar to the generic graph experiments, we do an ablation study on architecture sizes and apply the same learning rate schedulers. We choose the hyperparameters that exhibit the best score of the product between uniqueness and validation. We evaluate the generation results on 10000 generated molecules, measuring **Validity w/o correction** as the percentage of valid molecules without valence correction and edge resampling, **Uniqueness** as the percentage of valid molecules that is unique, and **Novelty** as the percentage of valid molecules not in the training set. Additionally, we compute two most salient metrics: Fréchet ChemNet Distance (**FCD**), measuring the distance in the chemical space between generated and training graphs, Neighborhood Subgraph Pairwise Distance Kernel (**NSPDK**) MMD, which measures the similarity of underlying structures between generated and test molecules. We present the detailed results in Table 7.

Novelty metric on QM9: Like DiGress (Vignac et al., 2023), our framework produces a low score on the novelty metric of QM9. However, the dataset comprises all enumerated small molecules that follow certain constraints. Hence, the generation of novel graphs beyond this dataset might not accurately reflect the model’s ability to capture the underlying data distribution.

Bridge prior ablation: We use the same set of hyperparameters as in the main experiment on QM9. In this study, we only retrain our bridge model with a new prior $\mathbb{P}_0 = \mathcal{N}(0, I)$. We provide the results in Table 7, where we can see that the change of prior has only marginal effect in the generation performance.

Quantisation ablation: In this experiment, we explore the effect of quantisation by removing the quantization step. This is still a discrete but non-quantised latent space which has the same dimensionality as the quantized latent space in the main experiment ($d_Z = 6$). We retrain both our graph autoencoder and the bridge model. However, the domain of graph latent structures is now non-quantised, denoted as $\Omega = [L_{\min}, L_{\max}]^{(n \times d_Z)}$, where L_{\min}, L_{\max} correspond to the minimum and maximum values of learned latent nodes for the entire training set. As per (Liu et al., 2023), the Π -bridge’s drift on a continuous domain is computed as:

$$\eta^h = \sigma_t^2 \nabla_{Z_t^h} \log \left(F\left(\frac{Z_t^h - L_{\min}}{\sqrt{\beta_T - \beta_t}}\right) - F\left(\frac{Z_t^h - L_{\max}}{\sqrt{\beta_T - \beta_t}}\right) \right), \quad 1 \leq h \leq (N \times d_Z) \quad (23)$$

where $Z_t \in [L_{\min}, L_{\max}]^{(n \times d_Z)}$, F is the standard Gaussian Cumulative Distribution Function (CDF). We provide the detailed results in Table 7. As we can see the removal of quantisation results to a drop in the generalisation performance as this is captured by NSPDK and FCD.

A.3. Visualizations

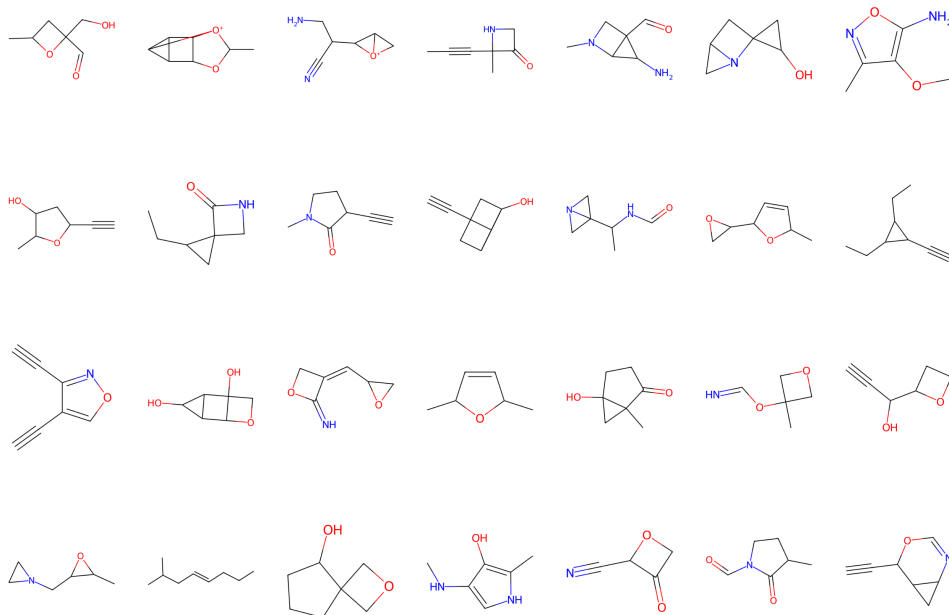
We provide the visualization of randomly generated molecules from QM9 in Figure 4, and from ZINC250k in Figure 5.

Table 6. **GLAD generation results on the generic graphs.** We show the means and standard deviations of 15 runs for each experiment.

	Deg.	Clus.	Orb.
COMMUNITY-SMALL	0.027 ± 0.018	0.044 ± 0.015	0.006 ± 0.004
EGO-SMALL	0.012 ± 0.007	0.013 ± 0.006	0.004 ± 0.002
ENZYMES	0.012 ± 0.004	0.014 ± 0.003	0.001 ± 0.000

 Table 7. **GLAD generation results on the molecule graphs, bridge prior and quantisation ablation.** Means and standard deviations of 3 runs on each dataset. ZINC250k and QM9 is standard GLAD, i.e. fixed prior and quantised discrete latent space. QM9* ablates the use of standard normal distribution for the bridge prior. QM9[†] ablates the effect of non-quantisation in the latent space.

	Validity \uparrow	Uniqueness \uparrow	Novelty \uparrow	NSPDK \downarrow	FCD \downarrow
ZINC250k	81.22 ± 0.00	100 ± 0.00	100 ± 0.00	0.002 ± 0.000	2.54 ± 0.04
QM9	97.24 ± 0.00	97.68 ± 0.00	39.54 ± 0.00	0.0003 ± 0.0000	0.222 ± 0.008
QM9*	95.38 ± 0.00	97.38 ± 0.00	41.54 ± 0.01	0.0004 ± 0.0000	0.330 ± 0.013
QM9 [†]	83.12 ± 0.01	97.54 ± 0.01	62.44 ± 0.53	0.0009 ± 0.0000	1.207 ± 0.003


 Figure 4. **Visualization of generated samples on QM9 from GLAD.**

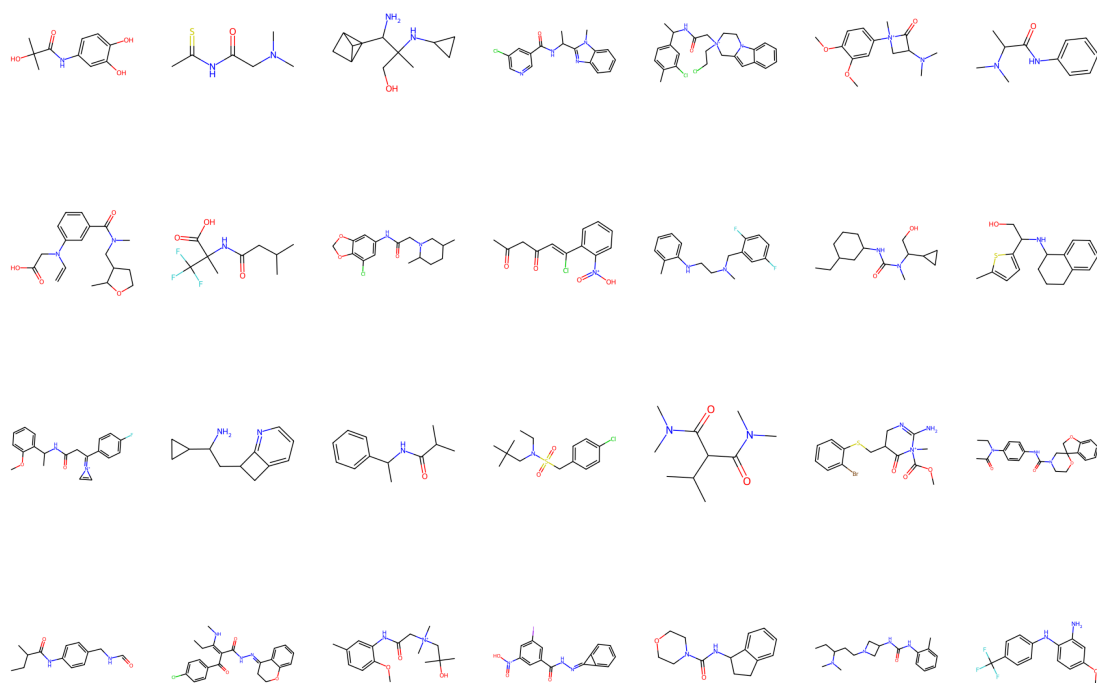


Figure 5. Visualization of generated samples on ZINC250k from GLAD.

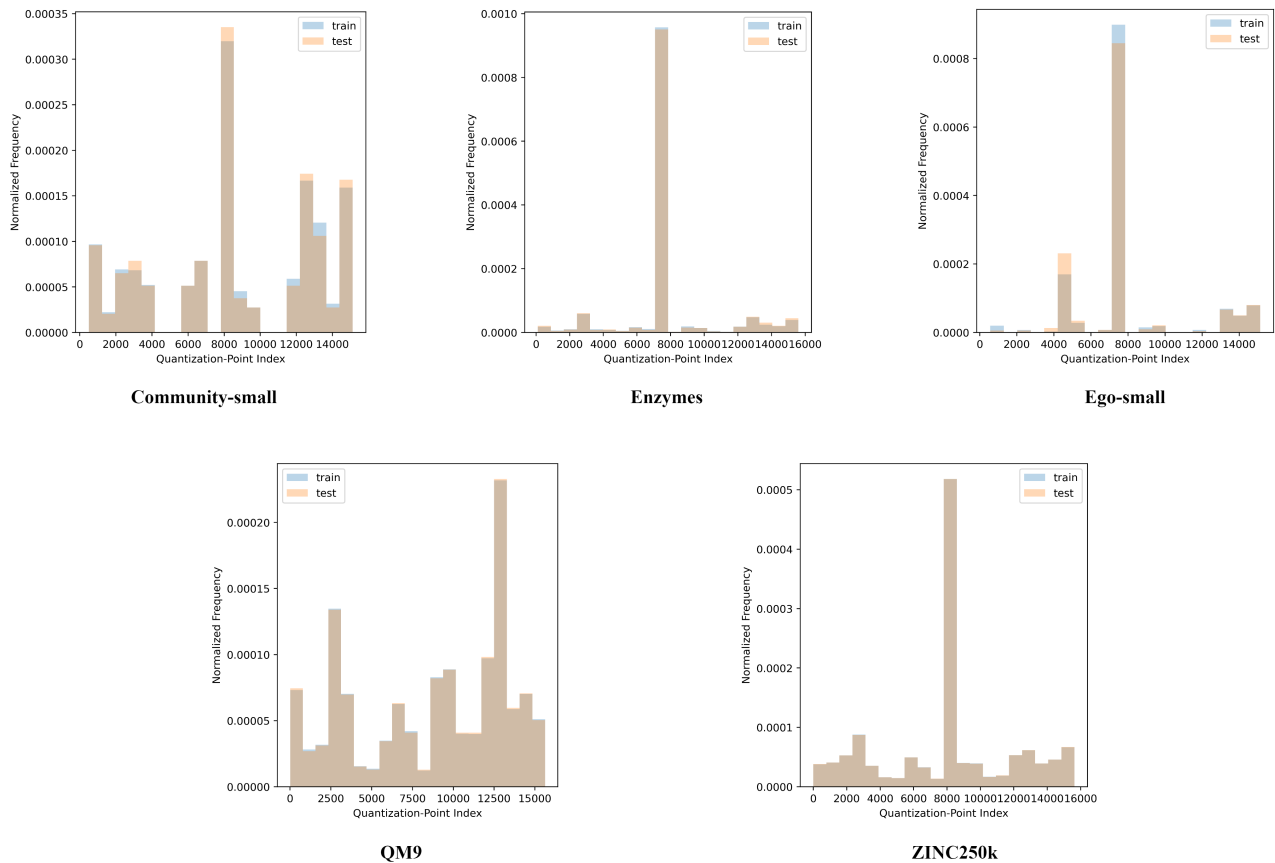


Figure 6. Visualisation of the distribution of number latent nodes per quantization point. We provide the distribution of latent nodes on the quantised latent space. For each dataset, we have $K = 5^6$ quantization points that are uniformly distributed in the latent space.

	Hyperparameter	Community-small	Ego-small	Enzymes	QM9	ZINC250k
ϕ	Number of heads	8	8	8	8	8
	Number of layers	8	8	8	8	8
	Hidden dimension X	256	256	128	256	256
	Hidden dimension E	128	128	32	128	128
	Hidden dimension Y	64	64	64	64	64
θ	Number of heads	8	8	8	8	8
	Number of layers	4	4	4	4	4
	Hidden dimension X	256	256	128	256	256
	Hidden dimension E	128	128	32	128	128
	Hidden dimension Y	64	64	64	64	64
f_ψ	Number of heads	8	8	8	8	8
	Number of layers	4	4	8	8	8
	Hidden dimension X	256	256	256	256	256
	Hidden dimension E	128	128	128	128	128
	Hidden dimension Y	64	64	64	64	64
SDE	σ_{\min}	1.0	1.0	1.0	1.0	1.0
	σ_{\max}	3.0	3.0	3.0	3.0	3.0
	Number of diffusion steps	1000	1000	1000	1000	1000
AE	Optimizer	Adam	Adam	Adam	Adam	Adam
	Learning rate	$5e^{-4}$	$5e^{-4}$	$5e^{-4}$	$5e^{-4}$	$5e^{-4}$
	Batch size	32	32	32	5240	512
	Number of epochs	3000	3000	3000	1000	1000
Model Bridge	Optimizer	Adam	Adam	Adam	Adam	Adam
	Learning rate	$[1e^{-4}, 5e^{-4}]$	$[1e^{-4}, 5e^{-4}]$	$[1e^{-4}, 5e^{-4}]$	$[1e^{-4}, 2e^{-3}]$	$[3e^{-4}, 2e^{-3}]$
	Batch size	64	64	64	1280	512
	Number of epochs	5000	5000	5000	2000	2000

Table 8. **GLAD hyperparameters**. We show the main training hyperparameters in the generic and molecule generation tasks. We provide the hyperparameters of the encoder ϕ , the decoder θ , the drift model f_ψ , the graph autoencoder training (AE), the model bridge training (Model Bridge), and the latent diffusion process (SDE).